

Simulation and Experiment of a Compact Wide-band 90° Differential Phase Shifter

Michał Sorn, Rafał Lech and Jerzy Mazur

Abstract—A compact wideband 90° differential phase shifter is developed by modifying ports termination in the Abbosh phase shifter configuration. This novel phase shifter arrangement consists of a 3 dB directional coupler with the coupled and transmission ports terminated with reactive loads. The proper reactance is found at the input of the coupled line section, in which the remaining ports are open circuited. Both coupled sections utilize a multilayer broadside coupling microstrip-slot-microstrip tight coupler. A theoretical model is presented to explain the performance of the proposed phase shifter and design procedure. Further, the phase shifter was designed and manufactured. Results of calculation and measurement show that the developed circuit provides a 90° differential phase shift with deviation less than $\pm 4^\circ$ across the 3 to 7 GHz frequency band.

Index Terms—phase shifters, broadside coupling couplers, band pass filters, ultra wideband technology.

I. INTRODUCTION

DIFFERENTIAL phase shifters are four-port passive microwave devices providing, in the specified bandwidth, a constant phase difference between the signals at their output ports. Ideally, such devices should produce proper phase shift values, exhibit relatively small attenuation and operate effectively over a wide frequency band. They are used, for example, in wide-band phased array antennas and find application in various microwave equipments and measurement systems. In principle, broadband phase shifters mainly use coupled lines sections. Schiffman [1] was the first who applied such a section to design an octave 90° differential phase shifter. This configuration included a reference transmission line and the two edge coupled striplines that were connected together at one end. When this circuit is fabricated in microstrip technology [2], [3], its operation deteriorates. The operation bandwidth decreases and deviation of the phase shift characteristic increases. These deteriorations are due to unequal phase velocities of the even and odd modes in the coupled microstrips. In recent years, one can find papers describing the design of modified phase shifter circuits with broader bandwidth, acceptable insertion losses and low phase shift deviation. These requirements are met in the circuits of the phase shifters proposed in [1]-[11], which used different arrangements of the edge coupled microstrip sections. In [1]-[4] the main circuit is designed as a cascade of the coupled

sections while in [6]-[8] the series or mixed connections are applied. These configurations provide acceptable phase shifter performance over a wide bandwidth greater than 100%. However, the insertion losses as well as the size of their circuits increase with increasing number of the interconnected sections.

The other arrangements proposed in [1], [9], [10] used the different configurations of the reference circuits instead of the transmission lines. The reference circuit is synthesized within a given frequency band in the way to obtain the parallel of the phase characteristic of the main section. The phase shifter reported in [9], [10] consists of both basic and reference circuits using edge-coupled lines sections of different electric lengths and the same coupling coefficients. Such arrangement provides narrowband performance, approximately 60% frequency band, as compared to the cascaded structures. The similar phase shifter structure previously was proposed in [1], where the reference edge coupled section was connected in series with the transmission line. The electric length of the main coupled section is three times longer than the coupled section applied in the reference circuit. The proper choice of the coupling coefficients of the main and reference coupled sections provides the acceptable phase shifter parameters over a wide frequency band, which is equal to about 100%.

A compact phase shifter proposed in [11] used the tapered coupled lines section to obtain a broader operating frequency band. The reported results indicated a bandwidth higher than 100%, which was better than those obtained for previously reported structures. However, the design of the phase shifters comprising edge coupled sections is limited by maximum coupling values of the edge coupled sections. The tight coupling requirements requires a very narrow slot between the coupled lines, which suggests difficulties in its fabrication in planar technology.

To improve the performance of the previously designed planar phase shifter, the compensation technique was introduced in [12]. It involves attaching a number of integrated capacitors to the phase shifter structure. This technique allows to improve only some properties of the circuit while others may deteriorate. The results indicate that the compensation improves the return loss performance while it increases the insertion loss and has no effect on the bandwidth of the circuit. Recently, Abbosh proposed a novel configuration of a phase shifter with broadband characteristics using a broadside microstrip-slot-microstrip coupler [13]. This type of coupler [14], [15] indicates good properties in the UWB band. Moreover, the coupler is characterized by tight coupling, which does not cause difficulties in its fabrication in comparison to the

Manuscript received ??????. The authors are with the Faculty of Electronics, Telecommunications and Informatics (ETI), Gdansk University of Technology (GUT), 80-952 Gdansk, Poland, e-mail: msorn@wp.pl, rlech@eti.pg.gda.pl, jem@pg.gda.pl

This work was supported under Polish Ministry of Science and Higher Education from sources for science in the years 2010-2012: partially under COST Action IC0803 (decision No 618/N-COST/09/2010/0) and under funding for Statutory Activities for ETI Gdansk University of Technology

edge coupled structure. In [13], an elliptical shaped broadside coupled structure was used to design a bandpass filter, which has been applied as a main coupled section of the phase shifter arrangement. The filter section is designed by open circuited coupled and transmitted ports of the broadside coupler. This approach allowed to design compact UWB phase shifters with the phase difference no larger than 48° .

Two simple planar structures of the differential phase shifters using basic high/low(H/L)-impedance transmission-line sections or coupled-line sections were presented and verified experimentally in [16]. The single H/L-impedance transmission-line section is useful to design 45° up to 90° differential phase shifters. Coupled-line section phase shifter can reach wide bandwidth for $90^\circ - 180^\circ$ differential phase shift with coupling coefficient level of $5.5 - 9$ dB. Loaded transmission lines are easily realized in microwave integrated circuit (MIC) and microwave monolithic integrated circuit (MMIC) technologies.

In [17], a simple configuration of the transmission line loaded with an open circuit is proposed to design a 90° phase shifter. The open circuit is designed as a T-shaped open stub. A good performance was achieved with insertion losses smaller than 0.6 dB and phase deviation $\pm 6.4^\circ$ over the frequency band $2.3 - 5.5$ GHz. A 45° broadband phase shifter employing a defect ground structure (DGS) under parallel stubs was proposed in [18]. In comparison to the phase shifter without DGS, the structure has wider bandwidth and smaller size. This configuration operates over a frequency range $2.2 - 6.1$ GHz with insertion loss and phase deviation within 2.2 dB and 3.3° , respectively. Another example of loaded transmission line phase shifter was proposed in [19]. The configuration makes use of non-radiating longitudinal slots in the broad wall of a substrate integrated waveguide (SIW) and allows to design a 90° phase shifter over a broad bandwidth from 21 GHz to 28 GHz.

With the rapid growth of MIC technology, the digital switched phase shifters become more popular [20], [21]. The switched phase shifters, as a key component in microwave digitally controlled modules and phased-array antennas, have been largely investigated in [20]. This configuration consists of a transmission-line branch and a bandpass filter branch. With this topology a 4-bit phase shifter was constructed with the use of 22.5° , 45° , 90° and 180° phase shifters. The measured performance showed the phase deviation less than 3.6° with the return loss larger than 15 dB from 1.06 to 1.95 GHz. In [21], a 45° dual-band phase shifter operating at 900 MHz and 1800 MHz was presented. The measured phase shift was $46.1^\circ \pm 2^\circ$ from 841 MHz to 930 MHz and $44.9^\circ \pm 2^\circ$ from 1743 MHz to 1924 MHz. The measured return loss was larger than 14.5 dB and 15 dB and the amplitude imbalances were smaller than 0.33 dB and 0.4 dB within the respective bandwidths.

This paper presents a new configuration of a broadside coupled 90° phase shifter consisting of two elliptical or rectangular shaped microstrip patches that are coupled through a slot in a common ground plane [14], [15]. The phase shifter is designed as a four-port coupler in which its two coupled and transmitted ports are terminated by reactive loads. The other

two ports are the input and output ports. Note, that the concept of this phase shifter is similar to that considered by Abbosh in [13], where these ports of the coupler were open circuited. However, this configuration provides small phase shifts and therefore, only the 30° and 45° phase shifters were reported in [13]. The proposed modification of the Abbosh phase shifter arrangement involving introduction of reactive loads allows to obtain larger phase shift values. A design procedure is presented using a simple scattering matrix model to optimize the proposed configuration of the designed phase shifter. The phase shifter frequency dependent return and insertion losses, frequency characteristics and frequency variation of the reactance load are calculated using this simple theoretical model. Finally, the proposed new design was simulated by the full-wave electromagnetic software ADS Momentum and validated by the measurement.

The comparison between different types and configurations of the phase shifters is presented in Table I. The planar configurations are better suited for MMIC technology while the configuration using broadside couplers are easily realized in multilayered PCB technology.

II. FORMULATIONS

The four port backward directional coupler with two of the output ports terminated by lossless reactance loads defined by reflection coefficient $\Gamma = e^{j\phi}$ is shown schematically in Fig. 1. Let us assume the coupler to be ideal [23] with coupling factor k_c . At the central frequency, its electrical length is $\theta_0 = 90^\circ$. For this coupler, the matching condition $Z_0 = \sqrt{Z^e Z^o}$ (Z_0 - port characteristic impedance, Z^e - impedance of even wave, Z^o - impedance of odd wave) and equalization of wave velocities $v^e = v^o$ is satisfied. As shown in Fig. 1, the coupled port (3) and transmitted port (4) of the coupler are loaded with Γ and ports (1) and (2) are assumed to be the input and output ports, respectively. Applying these assumptions to the scattering matrix equations of the ideal coupler [14], the reflection ($S_{11} = S_{22}$) and transmission ($S_{21} = S_{12}$) coefficients of the two port representing the phase shifter basis section are as follows:

$$S_{11} = S_{22} = \Gamma \frac{1 - k_c^2 (1 + \sin^2(\theta))}{\left(\sqrt{1 - k_c^2} \cos(\theta) + j \sin(\theta)\right)^2} \quad (1)$$

$$S_{12} = S_{21} = \Gamma \frac{j2k_c \sqrt{1 - k_c^2} \sin(\theta)}{\left(\sqrt{1 - k_c^2} \cos(\theta) + j \sin(\theta)\right)^2} \quad (2)$$

where θ is the electrical length of the coupled structure.

For the considered phase shifter, the differential phase shift is found as a difference between the phase of the signals that are transmitted through a basis coupled section ($\arg(S_{21})$) and reference line $\theta_L = (K\theta)$

$$\Delta\phi = K\theta - 2 \arctan\left(\frac{\tan(\theta)}{\sqrt{1 - k_c^2}}\right) + 90^\circ + \arg(\Gamma) \quad (3)$$

In (3) the electrical length is determined as $\theta = \beta_c l_c$ where β_c is the phase constant of the coupled structure and l_c is its physical length. For investigated structure we assume that

TABLE I
COMPARISON BETWEEN DIFFERENT TYPES AND CONFIGURATIONS OF THE PHASE SHIFTERS

type	configuration	phase shift $\Delta\phi$, bandwidth BW , insertion loss $L(\text{dB})$, max. deviation $\pm 3^\circ$	reference
Schiffman - single and multisection	1. Folded planar coupled line (CL) section $\lambda/4$	$45^\circ - 180^\circ, 3 : 1, < 1\text{dB}$	[1]-[3],
	2. Cascaded and stepped multisection of planar CL	$90^\circ, 180^\circ, 5 : 1, < 1.5\text{dB}$	[6]-[10],
	3. Tapered planar CL	$45^\circ, 5 : 1$	[11]
Schiffman CL section with opened and grounded stubs	1. Folded planar CL with two opened and grounded $\lambda/4$ stubs	$90^\circ, 180^\circ, 2 : 1$	[12]
	2. Folded planar CL with grounded planar CL stub	$180^\circ, 2 : 1$	[22]
Filters using transmission line (TL) or coupled line (CL) section	1. Broadside microstrip $\lambda/4$ coupler with two opened ports	$30^\circ, 45^\circ, 5 : 1, < 1\text{dB}$	[13]
	2. Broadside microstrip $\lambda/4$ coupler with two terminated ports by opened CL sections	$90^\circ, 2 : 1, < 1.5\text{dB}$	this study
	3. Planar open ended coupled microstrip $\lambda/4$ section of the bandpass filter and high/low transmission line filter (TLF)	$135^\circ, 2 : 1, < 1\text{dB}$	[16]
		$45^\circ, 2 : 1, 1\text{dB}$	
Loaded transmission line	1. Planar topology using microstrip line with T shaped open stub	$90^\circ, 2 : 1, < 0.6\text{dB}$	[17]
	2. Microstrip with parallel stubs using defected ground structure (DGS)	$45^\circ, 3 : 1, < 0.7\text{dB}$	
	3. Substrate integrated waveguide with non-radiating slots cut in the broad wall	$90^\circ, 1.5 : 1$	[19]
Digital switched phase shifters	1. Transmission line bandpass filter with single-pole-double-throw (SPDT) switches	4bit ($22.5^\circ, 45^\circ, 90^\circ, 180^\circ$), $2 : 1$	[20]
	2. Loaded transmission line with SPDT switches	45° , dual bandwidth	[21]

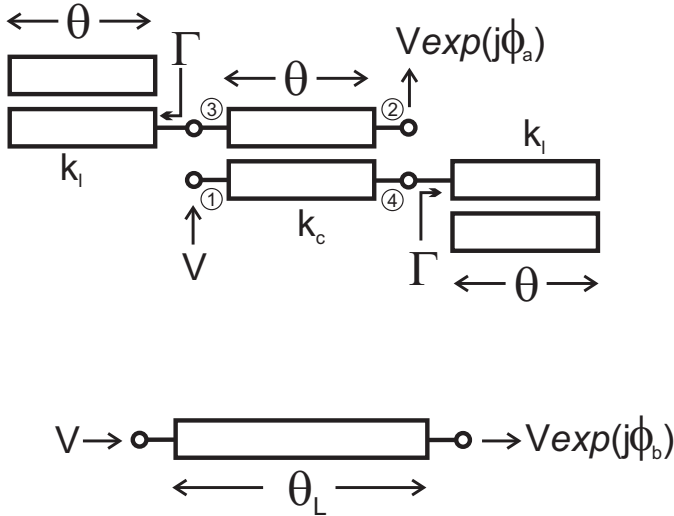


Fig. 1. Schematic representation of the proposed phase shifters

the propagation coefficients of even (e) and odd (o) modes are similar in value and therefore, it is possible to write that

phase constant $\beta_c = (\beta_e + \beta_o)/2$. The normalization coefficient $K = (\beta_L l_L)/(\beta_c l_c)$, where β_L is the phase constant and l_L is the length of the reference line. When the coupler and the reference line are designed on the same substrate and the phase constants $\beta_c \cong \beta_L$, the coefficient $K \cong l_L/l_c$ and it is independent of frequency.

Let us now introduce phase shift defined by equation (3) in the form of a sum of two partial differential phase shifts:

$$\Delta\phi = \Delta\phi_1 + \Delta\phi_2 \quad (4)$$

where

$$\Delta\phi_1 = K_1\theta - 2 \arctan\left(\frac{\tan(\theta)}{\sqrt{1 - k_c^2}}\right) + 90^\circ$$

$$\Delta\phi_2 = K_2\theta + \arg(\Gamma)$$

and $K = K_1 + K_2$.

The phase shift $\Delta\phi_1$ has the same form as reported in [13] for the phase shifter where two ports of the coupler are open circuited. When these ports are terminated by the reactive load, the phase shift $\Delta\phi_2$ is determined by the phase of the reflection coefficient $\Gamma = e^{j\phi}$.

Let us now consider the phase shifter configuration in which the main and the reference circuits are chosen as identical coupled sections. Two selected ports of the first section are terminated with reflection coefficient $\Gamma_1 = e^{j\phi_1}$ while in the second section with $\Gamma_2 = e^{j\phi_2}$. From (2) and (3), the differential phase shift is then determined by the phase difference of the reflection coefficients (i.e. $\Delta\phi = \phi_1 - \phi_2$). Using this method, it is possible to design a 180° phase shifter with a phase difference that is independent of frequency. It occurs when two ports in one section are short circuited ($\phi_1 = 180^\circ$) while in the second section they are open circuited ($\phi_2 = 0^\circ$).

The form of equation (4) properly defines the phase shift of the phase shifter consisting of cascaded two coupled sections. According to (4) the phase shift of the cascade is given by the summation of partial phase shifts produced by each section of this arrangement. Among these configurations are constructions of a 90° phase shifters [4]. The disadvantage of the cascade phase shifter configuration is its greater length than encountered in the other solutions. Therefore, the phase shifter configuration [13] modified by the change of termination of the ports of coupled line section might be an alternative design of the 90° phase shifter. For this phase shifter, the variation of the phase shift can be considered using (4) in the following form:

$$90^\circ = (\Delta\phi_{o1} + \delta_1(\theta)) + (\Delta\phi_{o2} + \delta_2(\theta)) \quad (5)$$

where, $\Delta\phi_{oi}$ for $i = 1, 2$, is nominal value of the phase shift while $\delta_i(\theta)$ is a deviation function from its nominal values. The reduction of the deviation magnitude is possible when variations of both deviation functions are similar but opposite in sign, so that $\delta_1(\theta) \approx -\delta_2(\theta)$.

In order to satisfy this condition, several reactive loads providing proper characteristics of the phase shifter were considered. The best performance was obtained using the structure shown in Fig. 1. The reactance is calculated as an input impedance of a four port section of coupled lines with three of its ports open circuited. The reflection coefficient at the input port of this coupled section with electrical length θ and coupling factor k_l , is found using (1) and (2) as:

$$\begin{aligned} \Gamma &= \frac{(\sqrt{1-k_l^2} \sin(\theta) + j \cos(\theta))^2}{k_l^2 \sin(\theta) - 1} = \\ &= -\exp\left(j2 \arctan\left(\frac{\cot(\theta)}{\sqrt{1-k_l^2}}\right)\right) \end{aligned} \quad (6)$$

Introducing (6) to (1) and (2), the scattering parameters of the main coupled section of the phase shifter are defined. From (6) results that k_l affects only the phase of the load reflection coefficient, which has a magnitude of 1. Then, the phase shifter insertion loss and return loss characteristics, defined by absolute value of the scattering parameters S_{11} and S_{12} , are independent of k_l . In this case, the insertion and return losses characteristics are the same as given for the phase shifter presented in [13]. It is worth noticing that their phase characteristics are different.

Now assume at the input of the phase shifter the tolerated value of the reflection coefficient Γ_m and denote the electrical

lengths θ_l , θ_u and θ_0 at the lower, upper and center frequencies of the operation band. Then we obtain from (1) the maximum return loss bandwidth of the phase shifter as:

$$\begin{aligned} BW_r &= \frac{\theta_u - \theta_l}{\theta_0} \Big|_{\theta_0 = \frac{\pi}{2}} = 2 - \frac{4\theta_l}{\pi} = \\ &= 2 - \frac{4}{\pi} \arccos \sqrt{\frac{|\Gamma_m| + 2k_c^2 - 1}{k_c^2 (|\Gamma_m| + 1)}} \end{aligned} \quad (7)$$

When the reflection coefficient $\Gamma_m = 0$, we obtain from (7) the coupling factor $k_c = 1/\sqrt{2}$. Considering transmission characteristics reported in [13], we note that the minimum value of insertion losses is obtained when the value of the coupling coefficient is chosen from the range (0.6 – 0.8). According to (1) and (7), such values of k_c provide the magnitude of the return loss better than 12 dB over the bandwidth $BW_r(\%) \in (30, 120)$.

To determine the differential phase shift $\Delta\phi$, the comparison is made with a reference line, which phase is defined by scaling its length coefficient K . From (3) and (6) it is formulated as

$$\begin{aligned} \Delta\phi &= K\theta - 90^\circ - 2 \arctan\left(\frac{\tan(\theta)}{\sqrt{1-k_c^2}}\right) + \\ &+ 2 \arctan\left(\frac{\cot(\theta)}{\sqrt{1-k_l^2}}\right) \end{aligned} \quad (8)$$

The value of K is estimated from (8) at the center frequency for coupling length $\theta_0 = 90^\circ$ as:

$$K = \left(\frac{2\Delta\Phi}{\pi}\right) + 3 \quad (9)$$

As we can see from (9), for 90° phase shifter the value of K is equal to 4. Using (8), the differential phase shift characteristics are calculated for the phase shifter. There is an odd symmetry of the $\Delta\phi(\theta)$ characteristics around the center length θ_0 . The value of the coupling factor $k_l = k_{lmin}$, for which the phase shift is constant around the θ_0 , is found from (8) by equating the first derivative of $\Delta\phi$ to zero at θ_0

$$k_{lmin} = \sqrt{1 - \frac{1}{(2 - \sqrt{1 - k_c^2})^2}} \quad (10)$$

Assuming the value of the coupling factor k_c of the main coupled section equal 0.74 and magnitude of $|\Gamma_m| = 0.1$ i.e. (–20 dB), the maximum return loss bandwidth BW_r calculated from (7) is equal to 79%. Variation of the phase shift with the electrical length θ is shown in Fig. 2 for different values of coupling factor k_l taken from the range of $k_l \in (k_{lmin}, k_c)$. The characteristic calculated for k_{lmin} shows the maximum flat and minimum magnitude of the phase deviation around the center length θ_0 . Considering the whole range of $\theta \in (0^\circ, 180^\circ)$, the smallest phase deviation is obtained for $k_l = k_c$. In this case, we can see in Fig. 2 that the two deviation amplitudes δ_1 and δ_2 (depicted on characteristics) have the same values. Their values are different, when $k_l \neq k_c$. Referring to Fig. 2, it is possible to choose the value of k_l that has an acceptable deviation δ_{max} over the phase shift bandwidth formulated by upper θ_{ϕ_u} and lower θ_{ϕ_l} electrical

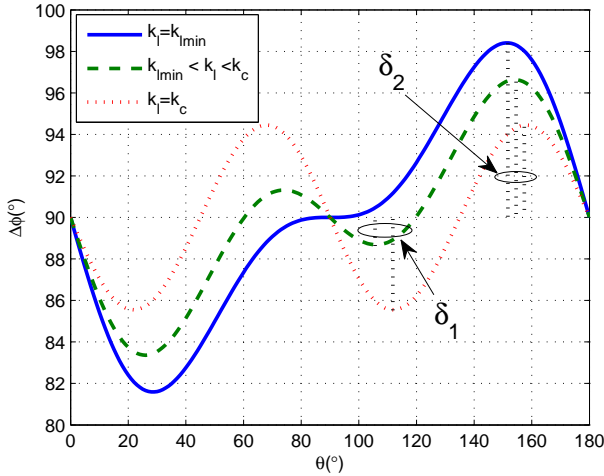


Fig. 2. Calculated phase shift characteristics of the phase shifter for different values of the coupling coefficients k_l . The coupling factor $k_c = 0.74$

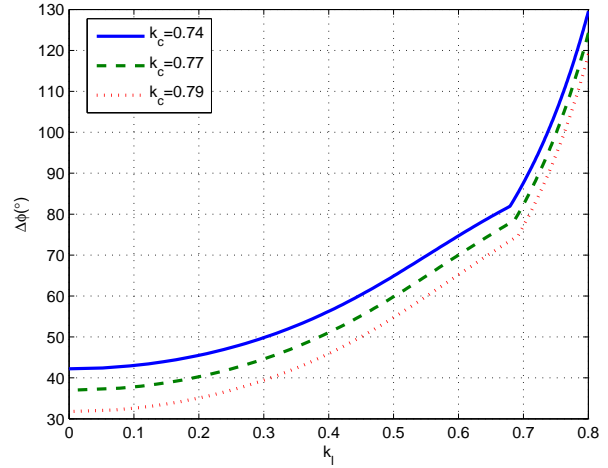


Fig. 4. Variation of the phase shift characteristics in dependence on coupling coefficient k_l for different values of coupling factor

lengths as $BW_\Phi = (\theta_{\phi_u} - \theta_{\phi_l})/\theta_0$. To illustrate this effect, we show in Fig. 3 the characteristics of δ_1 and δ_2 calculated versus coupling coefficient k_l . We observe that for $k_l < k_{lmin}$ the value of deviation δ_1 vanishes while the value of deviation δ_2 increases with decreasing k_l . Note, that the value of δ_2 has a great influence on the phase bandwidth BW_Φ when $k_l \leq k_c$. The situation is different for $k_l > k_c$ where we observe that $\delta_1 > \delta_2$. In this case the phase bandwidth BW_Φ is limited by value of δ_1 , which increases when k_l tends to 1. The rapid decrease of BW_Φ is observed in such case. From the above considerations, it is seen that the wide band of the phase shifter with acceptable deviation is achieved when the values of k_l are chosen from the range $\langle k_{lmin}, k_c \rangle$.

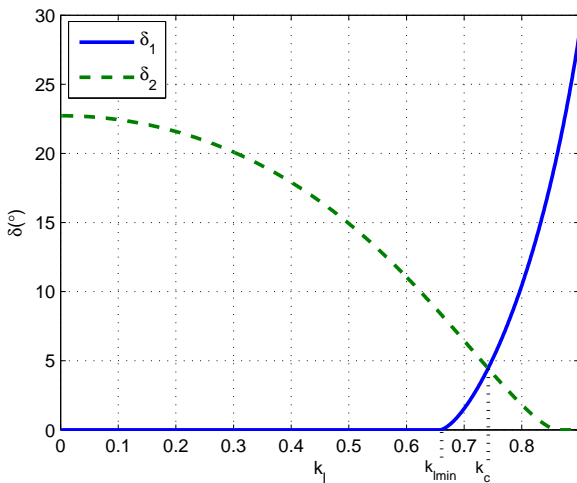


Fig. 3. Numerically estimated phase shift deviations depicted in Fig. 2 as δ_1 and δ_2 versus coupling coefficient k_l . The coupling factor $k_c = 0.74$

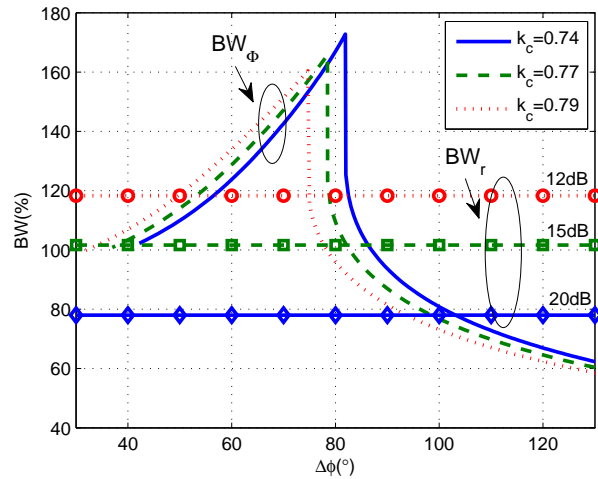


Fig. 5. Numerically estimated phase shift bands BW_Φ and return loss bands BW_r versus the nominal phase shift $\Delta\phi$ for different values of coupling factor k_c . The coupling factor $k_l = 0.7$

can be found when the value of coupling $k_c = 0.74$ and $k_l = 0.7$. The estimated magnitude of return loss using (1) is better than 20 dB. According to the results shown in Fig. 4, there is a direct relation between phase shift $\Delta\Phi$ and k_l while inverse dependence is observed between $\Delta\Phi$ and k_c . However, by choosing $k_c < 0.74$, the phase shifter return loss decreases. Fig. 5 shows the phase bandwidth estimated for different values of the phase shift. It can be seen that the wide bandwidth of the phase is achieved above 130% and below 150% when the phase shift is changed from 60° to 80°. For the designed 90° phase shifter, the phase bandwidth is equal to 90% but it is limited to the return loss frequency band equal to 80%. Figs. 6 and 7 shows the dependence of the phase shifter performance on the phase deviation. It is seen from Fig. 6 that there is a maximum of the phase band, which grows with the increasing of the deviation and it moves toward larger values

Variation of the phase shift $\Delta\Phi$ with k_l for different values of coupling k_c is shown in Fig. 4. Referring to Fig. 4, it is noted that the 90° phase shifter with $\pm 2^\circ$ deviation

of the phase shift. As it is apparent from Fig. 7, it is possible to design $90^\circ \pm 2^\circ$ phase shifter for the value of coupling coefficient $k_l \cong 0.7$. According to the results shown in Fig. 6, the operation frequency band of the phase shifter is limited to 80% band by the return loss assumed here to be better than 20 dB. Note that for both coupling sections, the values of their coupled factors decrease at the upper and lower frequencies of the operation band. Referring to Figs. 2 and 3, this effect will increase the phase deviation at those frequencies.

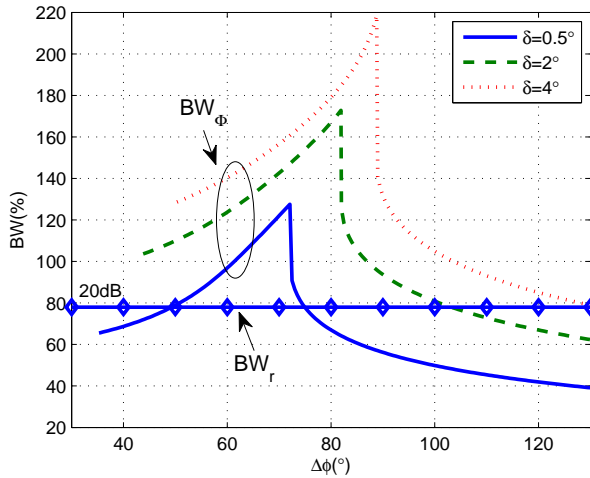


Fig. 6. Numerically estimated phase shift bands BW_Φ and return loss band BW_r versus the phase shift $\Delta\phi$ for different values of the phase deviation

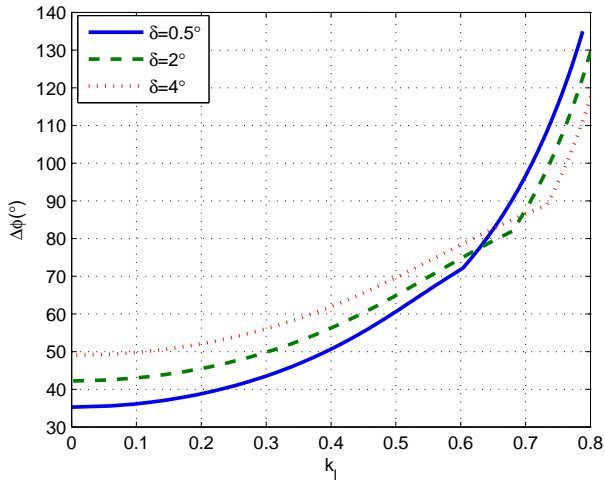


Fig. 7. Variation of the phase shift characteristics versus the coupling coefficient k_l for different values of the phase deviation

III. PHASE SHIFTER DESIGN AND RESULT DISCUSSIONS

To prove the validity of the proposed method, the phase shifter was designed using UWB integrated microstrip broadside coupled sections reported in [14] and [15]. The electrical length of both main and load coupled sections is equal 90° at the center frequency 5 GHz. Concerning $90^\circ \pm 2^\circ$ phase

shifter considered in the previous section, the main and load coupling sections are designed to ensure coupling factors equal $k_c \cong 0.74$ and $k_l \cong 0.7$ defined at the center frequency. For these parameters we can see from Figs. 5 and 6, that the return loss of the phase shifter can be better than 20 dB with bandwidth 80%. For the chosen central frequency the phase shifter should operate across the frequency band 3 – 6 GHz.

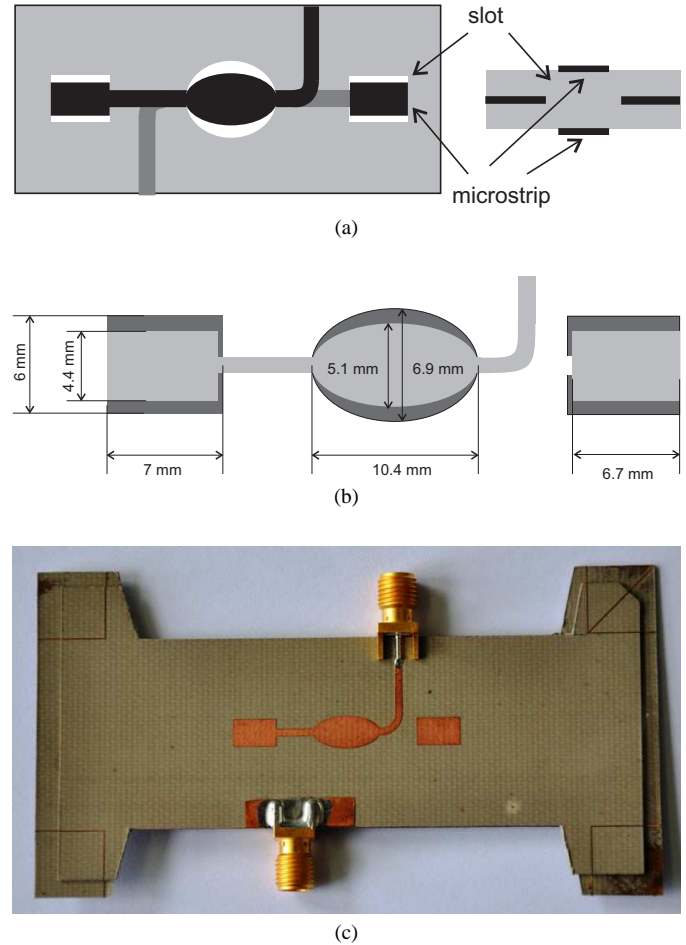


Fig. 8. Configuration of the proposed 90° phase shifter (a) schematic representation, (b) computed dimensions of the designed phase shifter circuit, (c) photograph of the manufactured phase shifter

The configuration of the phase shifter mentioned above is schematically shown in Fig. 8 together with the photograph of the manufactured prototype. The coupling sections of the proposed phase shifter utilize the elliptical [14] and rectangular [4] microstrip patches etched at the top and bottom layer and coupled through a slot. The shape of the slot is the same as microstrip patch and it is cut in the ground plane located at the mid of the structure. The configuration of the considered phase shifter were optimized and its characteristics were simulated using ADS Momentum. The designed phase shifter was manufactured using Taconic RF35 material with parameters: $\epsilon_r = 3.51$, $\tan \delta = 0.0018$, dielectric thickness 0.505mm and metallization thickness 0.017mm. The layers of the structure were joined with the use of glue with permittivity similar to the permittivity of the dielectric. The measurements of the manufactured phase shifter were

performed using vector network analyzer Wiltron 37269A. The simulated and measured results are presented in Figs. 9-10. Note, that the theoretically predicted overall performance of the considered phase shifter are confirmed by the results of the measurements. However, we can notice a small discrepancy

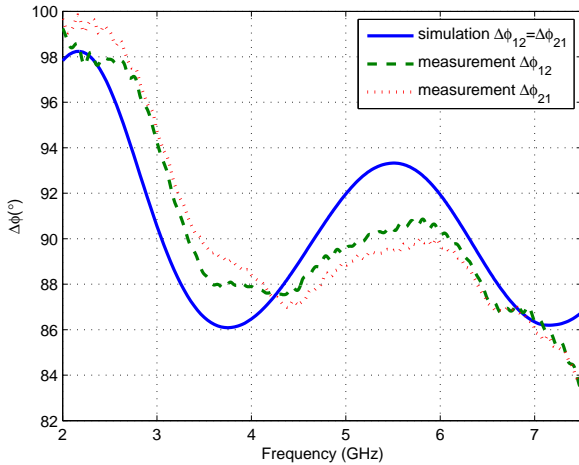
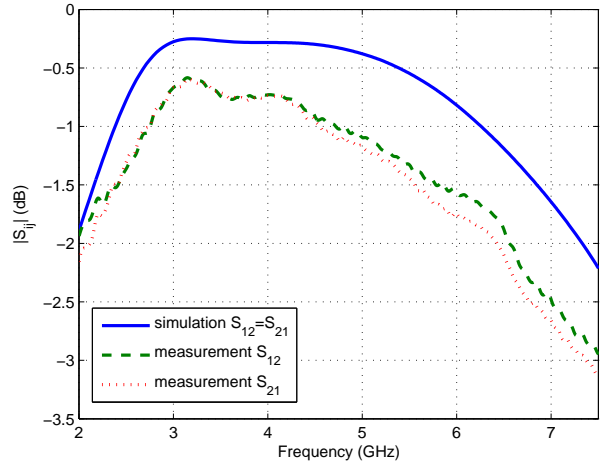


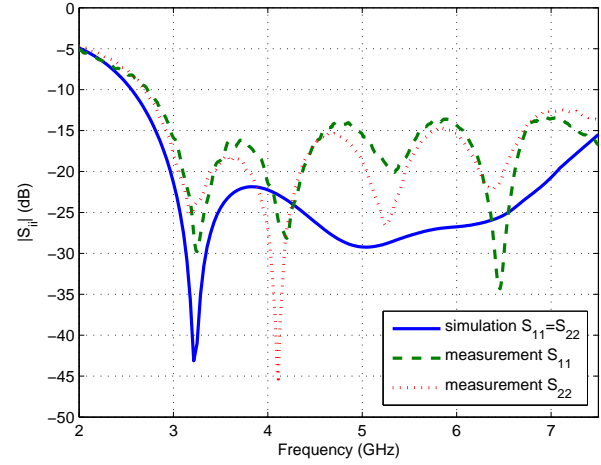
Fig. 9. Measured and simulated phase shift characteristics for the manufactured phase shifter

between the measured and simulated results. Both of them show the operation of the phase shifter across the 3 – 6 GHz band with the average differential phase shift equal 90° . The effect of the nonconstant value of coupling factors on phase deviation is observed in Fig. 9. The measured and simulated phase shift characteristics are similar, but the frequency shift about 0.2 GHz between them is observed. It is seen that the measured phase deviation is maximum around the center frequency in the 4.5 – 6.5 GHz band, and it is better than $\pm 3^\circ$ obtained from simulation. Both simulated and measured phase deviation increase to $\pm 4^\circ$ at the lower and upper frequencies of the operation band.

Measured and simulated results of the insertion and return losses are presented in Fig. 10. Note that the simulated insertion losses are better than 0.5 dB across the 3 – 5.5 GHz band, but around 6 GHz their values increase up to 0.8 dB as shown in Fig. 10a. The measured insertion losses are greater than simulated values by approximately 0.5 dB. This additional loss can be caused by the influence of the connectors, which are neglected in simulations and also by imperfection in fabrication of the phase shifter. There is also the differences observed in Fig. 10b between the return loss characteristics predicted by simulation and measured. The average measured return loss is 20 dB, and it is the same value as assumed for phase shifter design. As seen from the figure, the return losses are better than 15 dB in the considered 3 – 6 GHz band. Summarizing, the obtained measured and simulated results well confirm the feasibility of the proposed wide band 90° phase shifter which complement the family of the phase shifters reported in [13].



(a)



(b)

Fig. 10. Measured and simulated characteristic of the insertion and return losses for the manufactured 90° phase shifter

IV. CONCLUSION

The compact 90° phase shifter with wide band operation have been presented. The proposed configuration uses broadside coupling between two microstrip patches through the slot located in the common ground plane. The phase shifter properties are obtained by termination of two output ports of the coupled section with reactive load. The proper load, providing wide band operation of the phase shifter, was obtained as an impedance appearing at the input port of the directional broadside coupler where the other ports are open circuited. This configuration performance was analyzed using simple scattering matrix model of both coupled sections. The simple formulas have been proposed and used to design a 90° phase shifter. The designed phase shifter structure was optimized and simulated using ADS Momentum software. Despite the slight discrepancies between simulated and measured results, the obtained characteristics well confirm operation principles and design methodology of the proposed phase shifter. Moreover,

this configuration extends the class of the phase shifters proposed in [13]. Their broadside coupled configuration is preferable for implementation in multilayer integrated circuits.

REFERENCES

- [1] B. M. Schiffman, "A New Class of Broad-Band Microwave 90-Degree Phase Shifters," *IRE Trans. Microw. Theory Tech.*, vol. MTT-6, no. 4, pp. 232-237, Apr. 1958.
- [2] B. Schiek and J. Kohler, "A method for broad-band matching of microstrip differential phase shifters," *IEEE Trans. Microw. Theory Tech.*, vol. MTT-25, no. 8, pp. 666-671, Aug. 1977.
- [3] C. Free, C. Aitchison, "Improved analysis and design of coupled - line phase shifters," *IEEE Trans. Microw. Theory Tech.*, vol. 43, no. 9, pp. 2126-2131, Sept. 1995
- [4] B. M. Schiffman, "Multisection Microwave Phase-Shift Network," *IEEE Trans. Microw. Theory Tech.*, vol. 14, no. 4, pp. 209, Apr. 1966.
- [5] J. P. Shelton, J. A. Mosko, "Synthesis and Design of Wide-Band Equal-Ripple TEM Directional Coupler and Fixed Phase Shifters," *IEEE Trans. Microw. Theory Tech.*, vol. MTT-14, no. 10, pp. 462-473, Oct. 1966.
- [6] V. Meschanov, I. Metelnikova, V. Tupikin, and G. Chumaevskaya, "A new structure of microwave ultrawide-band differential phase shifter," *IEEE Trans. Microwave Theory Tech.*, vol. 42, no. 5, pp. 762-765, 1994.
- [7] Quirarte, J. Starski, "Synthesis of Schiffman Phase Shifters," *IEEE Trans. Microw. Theory Tech.*, vol. 39, no. 11, pp. 1885-1889, Nov. 1991.
- [8] B. Schiek, J. Kohler, "A Method for Broad-Band Matching of Microstrip Differential Phase Shifters," *IEEE Trans. Microw. Theory Tech.*, vol. 25, no. 8, pp. 666-671, Aug 1977.
- [9] J. Quirarte, J. Starski, "Novel Schiffman Phase Shifters," *IEEE Trans. Microw. Theory Tech.*, vol. 41, no. 1, pp. 9-14, Jan. 1993.
- [10] Yong-Xin Guo, Zhen-Yu Zhang, Ling Chuen Ong, "Improved Wide-Band Schiffman Phase Shifter," *IEEE Trans. Microw. Theory Tech.*, vol. 54, no. 3, pp. 1196-1200, Mar. 2006.
- [11] C. Tresselt, "Broadband tapered-line phase shift networks," *IEEE Trans. Microw. Theory Tech.*, vol. 55, no. 9, pp. 1935-1941, Sep. 2007.
- [12] S. Y. Eom, "Broadband 180° Bit Phase Shifter Using a $\lambda/2$ Coupled Line and Parallel $\lambda/8$ Stubs," *IEEE Microw. and Wireless Compon. Lett.*, vol. 14, no. 5, pp. 228-230, May 2004.
- [13] A. M. Abbosh, "Ultra-Wideband Phase Shifters," *IEEE Trans. Microw. Theory Tech.*, vol. 55, no. 9, pp. 1935-1941, Sep. 2007.
- [14] A. M. Abbosh, M. Bialkowski, "Design of compact directional couplers for UWB applications," *IEEE Trans. Microw. Theory Tech.*, vol. 55, no. 10, pp. 2262-2269, Oct. 2007.
- [15] W. Marynowski, A. Kusiek, A. Walesieniuk, J. Mazur, "Investigation of broadband multilayered coupled line coupler," *14th Conference on Microwave Techniques*, 2008. COMITE 2008, pp. 1-4, Apr. 2008.
- [16] P. Sobis, J. Stake, A. Emrich, "High/low-impedance transmission-line and coupledline filter networks for differential phase shifters," *IET Microw., Anten. Propag.*, vol. 5, no. 4, pp. 386-392, March 21 2011.
- [17] S. Y. Zheng, W. S. Chan, K. F. Man, "Broadband Phase Shifter Using Loaded Transmission Line," *IEEE Microw. Wireless Comp. Lett.*, vol. 20, no. 9, pp. 498-500, Sept. 2010.
- [18] S. Y. Zheng, W. S. Chan, K. S. Tang, K. F. Man, "Broadband parallel stubs phase shifter using defected ground structure," *Asia-Pacific Microwave Conference 2008, APMC 2008*, pp. 1-4, 16-20 Dec. 2008.
- [19] Z. Y. Zhang, K. Wu, and Y. R. Wei, "Development of broadband phase shifter using slotted substrate integrated waveguide structure," *IEEE International Conference on Ultra-Wideband (ICUWB)*, 2010, vol. 1, pp. 1-4, 20-23 Sept. 2010.
- [20] X. Tang, K. Mouthaan, "Phase-Shifter Design Using Phase-Slope Alignment With Grounded Shunt $\lambda/4$ Stubs," *IEEE Trans. Microw. Theory Tech.*, vol. 58, no. 6, pp. 1573-1583, June 2010.
- [21] X. Tang; K. Mouthaan, "Dual-band Class III loaded-line phase shifters," *Asia-Pacific Microwave Conference Proceedings (APMC)*, 2010, pp. 1731-1734, 7-10 Dec. 2010.
- [22] Gyu-Je Sung; Rahim Kasim; Jee-Youl Ryu; Bruce Kim, "Broadband 180° bit X-band phase shifter using parallel coupled lines," *European Microwave Conference, 2005*, vol. 3, pp. 4-6, Oct. 2005.
- [23] R. Mongia, I. J. Bahl, P. Bhartia, "RF and microwave coupled-line circuits", Artech House, 1999;



Michal Sorn was born in , Poland, in 1986. He received the M.Sc.E.E. degree from the Gdansk University of Technology (GUT), Gdansk, Poland in 2010.

His main research interests are phase shifters, numerical methods, electromagnetic modeling and filter design. He is currently employed at Intel Poland.



Rafal Lech was born in Elblag, Poland, in 1977. He received the M.Sc.E.E. and Ph.D. (with honors) degrees from the Gdansk University of Technology (GUT), Gdansk, Poland in 2001 and 2007, respectively.

His main research interests are electromagnetic-wave scattering, numerical methods, filter design, complex materials, metamaterial applications at microwave frequencies, electromagnetic analysis of periodic structures and conformal antenna design.



Jerzy Mazur was born in Brno, Czech Republic, in 1946. He received the M.Sc.E.E., Ph.D., and D.Sc. degrees from the Gdansk University of Technology (GUT), Gdansk, Poland, in 1968, 1976, and 1983, respectively. He received the title of Professor from the President of Poland in 1993.

He is currently a Full Professor with GUT. Since 1992, he has also been a consultant with the Telecommunication Research Institute, Poland. His research interests concern electromagnetic modeling of microwave and millimeter-wave integrated circuits, novel materials and their applications.

circuits, novel materials and their applications.

